Coverage dependence of adsorption-site geometry in the Cs/Ru(0001) system: A low-energy electron-diffraction analysis

H. Over, H. Bludau, M. Skottke-Klein,* and G. Ertl
Fritz-Haber-Institut der Max-Planck-Gesellschaft, Faradayweg 4-6, W-1000 Berlin 33, Federal Republic of Germany

W. Moritz
Institut für Kristallographie der Universität, W-8000 München 2, Federal Republic of Germany

C. T. Campbell
Department of Chemistry, University of Washington, Seattle, Washington 98195
(Received 13 November 1991)

The ordered overlayer structures formed by Cs adsorbed on a Ru(0001) surface were analyzed by use of low-energy electron diffraction (LEED). The phase diagram reflects the dominance of dipole-dipole repulsions between the adparticles and comprises quasiliquid configurations characterized by diffraction rings up to a coverage $\Theta=0.17$, followed by a (2×2) structure with maximum intensity of the diffraction spots at $\Theta=0.23$. Beyond $\Theta=0.25$, a series of structures with rotated unit cells is identified which are followed by a $(\sqrt{3}\times\sqrt{3})R30°$ structure around $\Theta=0.33$ ($\approx$completion of the first monolayer). In the (2×2) phase the Cs atoms are located in on-top sites with a Ru-Cs bond length of 3.25 ± 0.08 Å, corresponding to a hard-sphere radius of 1.9 Å for the Cs atom. In the $(\sqrt{3}\times\sqrt{3})R30°$ structure, on the other hand, the adatoms occupy threefold hollow hcp sites with Ru-Cs bond lengths of 3.52 ± 0.02 Å, corresponding to a Cs hard-sphere radius of about 2.2 Å. The increase in bond length and effective radius of the adparticle is paralleled by the transition of the character of bonding from more "ionic" at $\Theta=0.25$ (large dipole moment) to more "metallic" at $\Theta=0.33$ (dipole moment reduced by about 30%). The associated change of the type of adsorption site (from on-top to hollow) is qualitatively rationalized by a model according to which inherently less favorable sites may become preferred due to improved effective screening of the dipole-dipole repulsion by the location of substrate atoms in the region between neighboring adatoms.

I. INTRODUCTION

The adsorption site of a particle A on a single-crystal surface S is determined by the minimum of the A-S interaction potential which is corrugated parallel to the surface according to the two-dimensional periodicity of the substrate atoms. For atomic adsorbates, usually adsorption sites with high coordination (so-called hollow sites) are preferred.[1] At finite coverages adsorbate-adsorbate (A-A) interactions come into play, and the adsorption sites result from the combination of the A-A potential with the periodic potential of the substrate. As a consequence, multiple adsorption sites may be occupied such as, e.g., frequently identified with high-coverage CO adlayers.[2] Thus, for CO/Pd(111), the threefold hollow sites are energetically most favorable and are exclusively occupied at a coverage $\Theta=\frac{1}{3}$. At $\Theta=\frac{1}{2}$, however, adsorption is restricted to bridge sites, while at $\Theta=\frac{3}{4}$ both on-top and threefold sites are occupied.[3] (The various adsorbate geometries were, in these cases, identified somewhat indirectly by means of the vibrational spectroscopy probing the internal stretch frequency of the adsorbate.) These findings can be rationalized by the tendency for an uniform packing of the adsorbed phase. Thereby the total energy can be minimized despite the fact that less favorable sites also have to be occupied. This kind of interpretation is, however, based on the tacit assumption that the A-S and A-A interactions can be separated from each other and may simply be superimposed. Such a model may hold if the A-A interaction is much weaker than the strength of the bond between an isolated adparticle and the substrate surface. The present paper will describe the results of a structural analysis of an adsorbate system, Cs/Ru(0001), for which this approximation breaks down. The adsorption of alkali metals on transition-metal surfaces has been studied quite extensively in the past,[4,6] starting with the pioneering work of Langmuir.[7] With increasing coverage, the character of the chemisorption bond changes substantially as reflected by the nonlinear variation of the work function and by the varying bond length as derived for the system Cs/Ag(111) by means of surface extended x-ray-absorption fine structure (SEXAFS).[8] These effects are also qualitatively reproduced in recent theoretical treatments.[9,10] The strong variation of the adsorption energy with coverage is usually attributed to the operation of dipole-dipole repulsions, but indicates, on the other hand, that with such systems the energy of the single adparticle-substrate bond (A-S) no longer can be regarded to be much larger than the A-A interaction. Nevertheless, the interactions between the adsorbates can still be expected to be dominated by dipole-dipole repulsions (given by the square of the net dipole moment per adpar-

ticle as determined by the work-function change) over the whole range of coverages, leading to quasihexagonal configurations in which the A-A distances are maximized.[5]

These qualitative features are again retraced with the Cs/Ru(0001) system. More specifically, in the present work again a variation of the bond length between adparticle and substrate atoms with coverage was derived. But, even more remarkably, the adsorption sites also vary for reasons different from those holding for the quoted CO systems in which thereby sterically more favorable mutual adparticle configurations are reached: Cs atoms adsorbed on Ru(0001) form at $\Theta=0.25$ a (2×2) structure in which they occupy on-top sites, while with the $(\sqrt{3}\times\sqrt{3})R30°$ structure at $\Theta=0.33$ they are located in threefold hollow sites. These phases might well be formed with the adsorbate in *both* cases either in on-top or hollow sites without changing the A-A configuration and hence also the A-A interaction, provided that the latter can be viewed as decoupled from the A-S interaction—which is obviously not permitted.

II. EXPERIMENT

The measurements were performed in a UHV chamber (base pressure 7×10^{-11} mbar), equipped with a display-type four-grid low-energy electron-diffraction (LEED) optics and standard techniques for surface cleaning and characterization [Ar^+ sputtering, thermal desorption spectroscopy (TDS), Auger-electron spectroscopy (AES)]. The Ru(0001) sample (purity 99.99%), resistively heated via tungsten wires, was cleaned by argon-ion sputtering and oxidative removal of surface carbon (details of the cleaning procedure are given, e.g, in Ref. 11). After a final heating to 1540 K for a few seconds in order to desorb excess oxygen, the sample exhibited a LEED pattern with sharp spots and low background intensity. The crystal temperature, measured by a thermocouple which was spotwelded to the rear side of the crystal, could be varied between 80 and 1540 K.

Cesium was evaporated from a well-outgassed dispenser source (SAES getters, Inc.) at a typical rate of about 0.5 monolayers per minute. The Cs coverages were calibrated by using the integrated TD spectrum of an overlayer showing a $(\sqrt{3}\times\sqrt{3})R30°$ LEED pattern with optimum intensity. This phase was assumed to represent a coverage of 0.33. The coverage Θ is defined as the ratio of the number of adsorbate atoms to top-layer substrate atoms. This calibration was confirmed by the (2×2) structure which exhibits its highest intensity at $\Theta=0.23$, close to the nominal value of 0.25.

In order to establish varying defined submonolayer coverages, the sample was first covered with about two monolayers of Cs ($T_{\text{sample}}=200$ K) and then heated up to certain temperatures to desorb excess cesium. The uncertainty in the temperature leads only to a small uncertainty in coverage because of the strong temperature dependence of the onset of desorption as a function of coverage as reflected by the large width of the submonolayer thermal desorption spectra.

LEED intensity measurements were performed at normal incidence of the primary beam at a sample temperature of 100 K. A computer-controlled video camera was used to record integrated spot intensities from the fluorescence screen.[12] Normal incidence was adjusted using the I-E curves of symmetry equivalent beams. All I-E curves were background corrected and normalized to a constant incident beam current. After averaging the curves of symmetry equivalent beams, they finally were deconvoluted concerning Lambert's law, in order to compensate the change in luminosity as the LEED pattern is projected onto a plane.

The Cs-covered surface exhibits a high sticking coefficient for oxygen, and therefore much care was taken to minimize such spurious effects. For example, the I-E curves of the different beams for the two phases analyzed were recorded in varying sequence, without noticeable difference as long as the total period for measuring was kept below about 1 h.

In addition, several control experiments were performed in which the Cs-covered surface was purposely exposed to a gas atmosphere. It turned out that small doses of oxygen [0.05 L (1 L$=1.33\times10^{-6}$ mbars)] adsorbed on the $(\sqrt{3}\times\sqrt{3})R30°$ structure already lead to the appearance of a new superstructure and a successive disappearance of $(\sqrt{3}\times\sqrt{3})R30°$ beams.[13] The adsorption of CO, which is always present in the residual gas, required much higher exposures (>6 L) in order to induce a change in the LEED pattern. No influence on the I-E curves could be observed for exposures from the residual gas within the measuring time.

For the (2×2) phase, we found that, after exposing the Cs-covered sample to small amounts of oxygen (<0.05 L), the half-order spots sharpened significantly, implying a stabilization of the long-range order of the Cs layer. A similar observation was reported by Chandavarkar and Diehl[14] for the (2×2) phase of K/Ni(111). However, small amounts of oxygen did not affect the measured I-E curves, indicating a stable local geometry of the Cs adsorbate.

III. CHARACTERIZATION OF THE Cs/Ru(0001) SYSTEM

The Cs/Ru(0001) system has already been the subject of several investigations.[15,16] Previous TDS, AES, $\Delta\phi$, and LEED observations were essentially confirmed in the course of the present study. Although the main emphasis of this paper will be put on the LEED structure analysis, some new experimental results and others deviating from previous investigations will be presented in this chapter.

Figure 1 shows a series of thermal desorption spectra taken for various initial Cs coverages. The spectra are similar to those reported by Hrbek,[15] but there is a difference in identifying the multilayer desorption peak. The spectra show a broad desorption peak, labeled by α, which saturates at the first monolayer coverage, corresponding to the optimum $(\sqrt{3}\times\sqrt{3})R30°$-Cs structure with $\Theta=\frac{1}{3}$. For higher coverages, a narrow peak (γ) appears, which in our experiments saturates at a coverage of 0.58 (±0.02). Still higher coverages desorb in a multilayer desorption peak at even lower temperature. So that second layer of cesium turns out to be distinguishable in

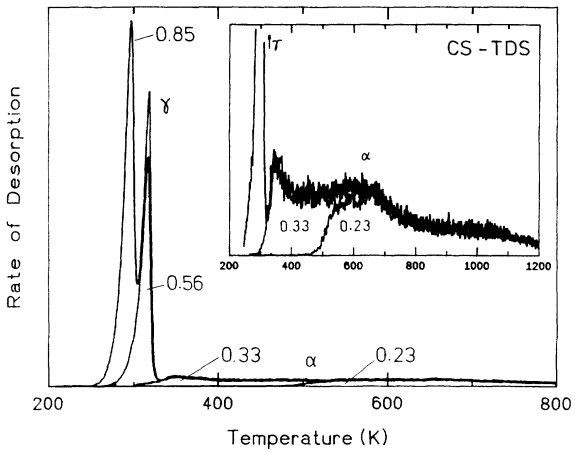

FIG. 1. Series of thermal desorption spectra for different initial coverages of Cs on Ru(0001). The heating rate values 5.4 K/s. For clarity the inset shows the α peak in a magnified representation. The numbers are representing the initial Cs coverage (with respect to the substrate).

TDS. The saturation coverage of the second layer is $0.58-0.33=0.25$. This value corresponds to a mean interatomic spacing between Cs atoms of 5.39 Å, which is very close to the Cs bulk value of 5.38 Å.[16] An analysis of the leading edges of the multilayer and second-layer desorption peaks yields activation energies for desorption of 72 ± 7 and 81 ± 7 kJ/mol, respectively. For comparison, the value for Cs bulk sublimation is 78.9 kJ/mol.[17] The different activation energies for desorption responsible for the appearance of distinguishable desorption peaks obviously have their origin in the influence of the substrate which extends to the second Cs layer. An alternate view attributes this difference to the interaction of the second-layer atoms with those of the first layer in which the Cs atoms are closer together than in bulk cesium and exhibit not yet fully their metallic character.

Figure 2 shows the experimentally derived (T,Θ) phase

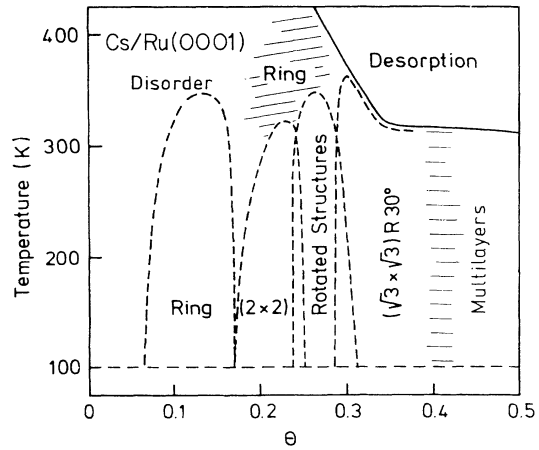

FIG. 2. Experimental phase diagram for Cs/Ru(0001). The dashed line separating the $(\sqrt{3}\times\sqrt{3})R30°$ from desorption is due to the experimental limitation to temperatures below desorption temperature. The hash-marked area represents a qualitative result.

diagram for the system Cs/Ru(0001). The Cs coverages were determined by integrating the corresponding TD spectra. The phase boundaries were constructed from the turning points of the intensities of the corresponding LEED superstructure spots as a function of temperature. The rich variety of phases is typical for adsorption systems with repulsive lateral interactions and has similarly been found in other alkali-metal adsorption systems, such as Na/Ru(0001),[18] K/Pt(111),[19] K/Ni(111).[14] The corresponding one-dimensional sequence of phases as a function of coverage (at fixed temperature) is similar to that reported by Hrbek,[15] except for the observations in the intermediate coverage region between the two commensurate structures. For low coverages the typical alkali-induced ring structure is observed, with the ring diameter being a function of coverage. The ring indicates a liquidlike structure with a constant mean spacing between the adsorbate atoms and no azimuthal ordering with respect to the substrate. With increasing coverage, the (2×2) phase develops with maximum intensity of its half-order beams at $\Theta_{Cs}=0.23$. This phase is stable up to 325 K. Upon increasing the temperature, a transition from the (2×2) phase to disorder proceeds through a range characterized by a ringlike diffraction pattern intersecting the $(\frac{1}{2},0)$ position. This indicates that the dipole-dipole interaction is still sufficient to force the Cs atoms in a constant interatomic spacing, while the azimuthal ordering by the corrugation of the substrate is weaker and hence lifted first.

The transition to the $(\sqrt{3}\times\sqrt{3})R30°$ structure takes place via a phase regime denoted as "rotated structures" which shows two small coexistence regions. The $(\sqrt{3}\times\sqrt{3})R30°$ structure is the phase with the highest thermal stability. It can be observed up to desorption temperature.

We now concentrate on the intermediate coverage region between the two commensurate structures. A typical LEED pattern is shown in Fig. 3 ($\Theta_{Cs}=0.27$, $E=55$ eV) together with a sketch including a possible unit cell in reciprocal space.

In principle, there are different ways how an overlayer transforms from one commensurate phase to another: via a disordered phase, via formation of antiphase domains, or through a rotational transition (observed, e.g., with several physisorbed noble gases on graphite[20,22] and alkali-metal systems).[23,24] All efforts to construct a model structure containing antiphase domains failed; no model could be found leading to spot splitting as shown in Fig. 3. The only plausible interpretation of this structure is based on the existence of a rotated unit cell (see Fig. 3). In addition, double-scattering spots are required. The streaky shape of the fractional order beams is then a consequence of a slight orientational disorder of the Cs layer. The continuous spot splitting as a function of coverage becomes evident from the series of intensity profiles shown in Fig. 4. The angle of rotation decreases slightly with increasing coverage from 9° to 7°, while the length of the unit-cell vectors decreases in quantitative correlation with the respective coverage, indicating a fully relaxed Cs layer.

Translation of these observations into real space leads

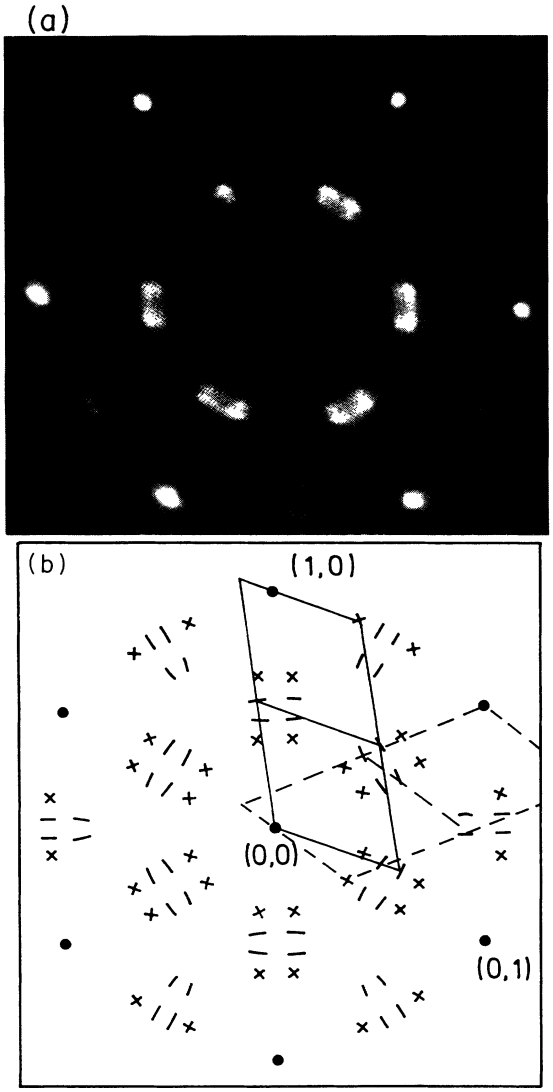

FIG. 3. Photograph of the LEED pattern for $\Theta_{Cs}=0.27$ ($E=55$ eV) together with a schematical picture. For clarity, only one of the possible unit cells (solid lines) and corresponding unit cells due to double scattering (dashed lines) is inscribed. Weak spots are marked by crosses.

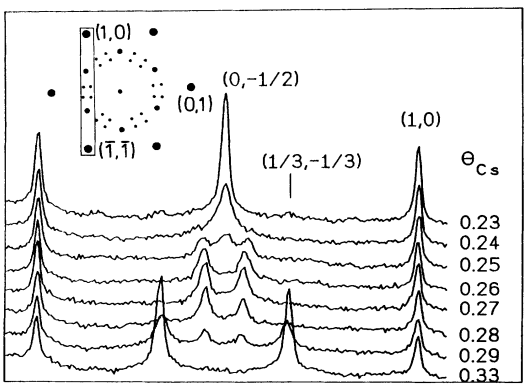

FIG. 4. Profiles as a function for coverage, showing the development of the LEED pattern from the $(\sqrt{3}\times\sqrt{3})R30°$ phase to the (2×2) phase.

to the conclusion that the repulsive lateral interactions between the adsorbate atoms are strong enough—if compared to the corrugation of the potential derived from the adsorbate-substrate interaction—to prevent the Cs atoms from locking in at highly symmetric adsorption sites. On the other hand, no continuous rotation, as predicted by the theory of Novaco and McTague[25,26] and experimentally observed for the system Na/Ru(0001),[24] can be found in the Cs/Ru(0001) system. The "rotated structures" of the presented system exhibit only a limited rotation angle around 8°. The LEED patterns presented by Duszak and Prince[27] for the intermediate coverage region of Cs/Ru(0001) indicates the formation of (2×2) antiphase domains. However, these patterns were caused by coadsorption of oxygen, as will be described in detail elsewhere.[13]

IV. CALCULATIONAL PROCEDURES

The LEED intensity calculations were performed using the "layer doubling method" in connection with the "layer KKR" (Korringa-Kohn-Rostoker) approach.[28] Particular attention was paid to exploit symmetrization in plane-wave[29] as well as in angular momentum representation[30] of the wave field. The crystal potential for ruthenium was calculated relativistically by overlap from free-atom potentials using Slater's exchange term with Schwarz's optimized α parameter.[31] The corresponding Ru phase shifts were computed relativistically.[32] In the LEED program, nine spin-averaged phase shifts were used. In a similar procedure the nine Cs phase shifts were evaluated, the superposition of the free-atom potentials were performed by arranging Cs in a bcc matrix with a lattice constant corresponding to that of metallic cesium. The thermally induced vibrations of atoms were taken into account within the framework of the Debye-Waller approximation. For the Ru layers, a Debye temperature of $\Theta_D^{Ru}=420$ K (Ref. 33) was used; the corresponding bulk value for cesium is 38 K.[33] Since all I-E data were measured at 100 K, a strong influence of Θ_D^{Cs} on the r factor was expected. Therefore, the Debye temperature of cesium had to be refined additionally. As a further, nonstructural parameter, the real part of the inner potential was included in our analysis.

The agreement between experimental and theoretical intensity data was quantified by the r_{DE} factor introduced by Kleinle *et al.*[34] and by Pendry's r factor r_P.[41] Besides a small data set of data points at discrete energies required for the r_{DE} factor, the main advantage is that it allows one to apply nonlinear least-squares optimization procedures for simultaneous refinement of structural and nonstructural parameters.[35] This method requires the computation of partial derivatives of the intensities with respect to each parameter to be optimized. In the program version of Kleinle,[36] in the following, in short, called "exact version," this gradient is evaluated numerically by full-dynamical calculations. A significant improvement in computing economy can be achieved by computing the derivatives in a linear approximation scheme,[37] which has been partially used here. The calculation for the intensities for incremented structural pa-

rameters is performed in two steps according to the corresponding LEED intensity calculation starting with the evaluation of the scattering matrices of each composite overlayer and the following stacking by the layer doubling scheme. A full description will be given elsewhere.[38]

The diffraction pattern of the clean Ru(0001) surface exhibits a quasi $p6mm$ symmetry, although an ideal hcp (0001) surface has only $p3m1$ symmetry. Since the basal plane of a hcp structure with its $ABABAB\cdots$ layer sequence can be terminated either by an A or a B plane, the $p6mm$ symmetry of the diffraction pattern is a result of a statistical distribution of both types of domains; note that both terminations can be transformed to each other by a 60° rotation. Provided the domain sizes are large enough, the I-E curves to be compared with the experimental data are then obtained by intensity superposition.

V. RESULTS OF THE LEED ANALYSIS

A. The clean Ru(0001) surface

As a test of our new video-LEED apparatus, the clean Ru(0001) surface was reexamined, which had already been analyzed before.[39] For comparison with model calculations, three LEED spots of Ru(0001) were investigated in the energy range between 70 and 380 eV. The step width of 10 eV corresponds to 31 points on the energy scale, yielding a total number of 86 data points. This data base was by far sufficient to determine both the first and second Ru layer spacing as well as the real part of the muffin-tin zero. Starting from the truncated bulk structure, the automatic fit procedure converged rapidly. Final results were attained after four iteration cycles with all parameters within limits of 0.01 Å and 0.1 eV, respectively. A comparison between the "exact version" and the linear approximated counter part indicated a very similar behavior in convergence; the latter procedure caused a reduction in computing time for this simple system by 45%. The findings of this analysis are the following.

The clean Ru(0001) surface is unreconstructed and its first-layer spacing is slightly contracted as compared to the bulk value ($D_{12}=2.09\pm0.02$ Å instead of 2.14 Å); the inner potential has a value of -8.0 ± 0.1 eV. For this structure the corresponding r factors are

$$r_{DE}=0.21\ ,\ r_{ZJ}=0.07\ ,\ \text{and}\ r_{P}=0.18$$

(ZJ for Zanazzi and Jona,[40] P for Pendry[41]). These results agree very well with corresponding data obtained previously by Michalk *et al.*[39]

B. The Cs $(\sqrt{3}\times\sqrt{3})R30°$ structure

In the hard-sphere model, the lower bound for the Cs radius is given by the Pauling radius of Cs^+ (Ref. 42) of 1.7 Å. As a consequence, the unit cell of the Cs$(\sqrt{3}\times\sqrt{3})R30°$ phase has to contain a single adparticle, corresponding to a Cs coverage of 0.33. Four distinguished highly symmetric adsorption sites had been considered in this analysis: in addition to the on-top position, the cesium atom had been put in the twofold symmetric bridge position and above the two possible (fcc and hcp) threefold hollow sites; the corresponding symmetries were pm for the bridge site and $p31m$ for the on-top and hollow sites.

In the optimization procedure, the Cs-Ru layer spacing, the first two Ru-Ru layer spacings, and a buckling in the first or second Ru layer depending on the Cs adsorption site were simultaneously refined. Alternatively, lateral relaxations in the first Ru layer could be included in our LEED structure analysis. The experimental data set comprised three integer and three fractional-order LEED spots in the energy range between 70 and 380 eV.

In order to determine the Cs adsorption site, in a first stage only the Cs-Ru and the first Ru-Ru layer spacing as well as the real part of the muffin-tin zero were refined. With a step width of 10 eV on the energy scale, a total number of 77 data points in 6 beams were used for comparison with the experiment. The Debye temperature for Cs was kept fixed at 50 K. Depending on the starting configuration (Cs-Ru layer spacing), the optimizing scheme reached various local minima in the r_{DE} factor surface. The optimum layer spacings and the r_{DE} factor for the respective Cs adsorption sites are compiled in Table I. The on-top site can be clearly ruled out; among the other three adsorption sites, the r_{DE} factor of 0.318 gives a significant preference for the hcp site with its optimal layer spacings $Z_{Cs}=3.16$ Å and $D_{12}=2.10$ Å.

In the second stage of analysis, additional variations of the Debye temperature of Cs and small lateral and vertical relaxations of the substrate were included. For this purpose, the step width of the energy scale was reduced to 5 eV, corresponding to an increased data set of 181 energy points. This energy grid also permitted calculation of the standard r factors, as introduced by Zanazzi and Jona[40] and by Pendry,[41] respectively. As a consequence of the enlarged data set, all r_{DE} factors increased nearly uniformly for the different models by about 0.06, however, without affecting the preference of the hcp site.

Lateral relaxations of the substrate compatible with threefold symmetry, namely, symmetric rotation and contraction of three adjacent Ru atoms, led to no improvement of the associated r_{DE} factors. Moreover, a la-

TABLE I. r_{DE} factors (step width 10 eV) and structural parameter for the best-fit arrangement of the respective Cs adsorption sites [$(\sqrt{3}\times\sqrt{3})R30°$].

r_{DE}	Z_{Cs} (Å)	D_{12} (Å)	Adsorption site
0.352	3.88	2.10	hcp
0.318	**3.16**	**2.10**	**hcp**
0.396	2.66	2.09	hcp
0.529	3.27	2.10	On top
0.588	3.94	2.12	On top
0.396	2.74	2.09	Bridge site
0.380	3.13	2.10	Bridge site
0.396	2.66	2.09	fcc
0.414	3.14	2.13	fcc

teral displacement of 0.08 Å turned out to worsen the agreement and was placed back during the fit procedure. Independent of the Cs adsorption site, the Debye temperature of cesium, on the other hand, decreased during the optimizing procedure for the various adsorption sites to a value of 30 K which is below that of the bulk (38 K). The r factors for the best fit of the various Cs adsorption sites are collected in Table II. They again exhibit a pronounced preference for the hcp site; nevertheless, Pendry's r factor with a value of 0.50 indicates only fairly poor agreement between experiment and theory.

Next, we will discuss the reliability of the LEED program, applying the linear approximation. As an example, an automatic structure refinement of the model with Cs located at the hcp site and the simultaneous optimizing of eight parameters, namely, the Ru-Cs and the first two Ru-Ru layer spacings, a buckling in the second Ru layer, a contraction and rotation of three adjacent Ru atoms in the first layer, the real part of the muffin zero, and the Debye temperature of Cs, was performed (note that, for symmetry arguments, in this case there can be no buckling in the first Ru layer). Final results were attained after six iteration cycles when all parameters were within the limits of 0.01 Å, 0.1 eV, and 0.5 K, respectively. A comparison with the exact version indicated the same behavior of convergence but with reduction of computing time by a factor of 2.8.

The serious problem concerning the poor agreement between experimental and theoretical I-E curves which is reflected by $r_P = 0.50$ was still unresolved. Therefore, we varied within a grid search the Debye temperature Θ_D^{Cs} of Cs between 40 and 140 K, including small variations of the Ru-Cs and the first Ru-Ru layer spacing. The results of the calculations are summarized in Fig. 5, which shows both the r_{DE} and the r_P factors as a function of Θ_{Cs}^D. As a striking result, the r_P factor runs through a pronounced minimum located at 80 K, while the r_{DE} factor remains nearly constant with $r_{DE} = 0.400 \pm 0.015$. Similar tests were performed for the other adsorption sites but no significant improvement could be achieved. A comparison of I-E curves for various Cs Debye temperatures shows clearly why the r_P factor decreases drastically with increasing Θ_D^{Cs}.

In particular, with the fractional order beams some "small" single peaks change into double structures which fit better to the experimental data and give rise to smaller values of r_P. On the other hand, the intensities of some peaks in integer order beams are less well reproduced, so that these two effects cancel each other with respect to the r_{DE} factor.

TABLE II. r factors (r_{DE}, Zanazzi-Jona's r_{ZJ}, and Pendry's r_P; step width 5 eV) for the best-fit arrangement of the respective Cs adsorption sites, optimized Debye temperature of Cs 30 K [$(\sqrt{3}\times\sqrt{3})R30°$].

r_{DE}	r_{ZJ}	r_P	Adsorption site
0.390	0.14	0.50	hcp
0.530	0.22	0.65	On top
0.510	0.27	0.68	Bridge site
0.590	0.30	0.70	fcc

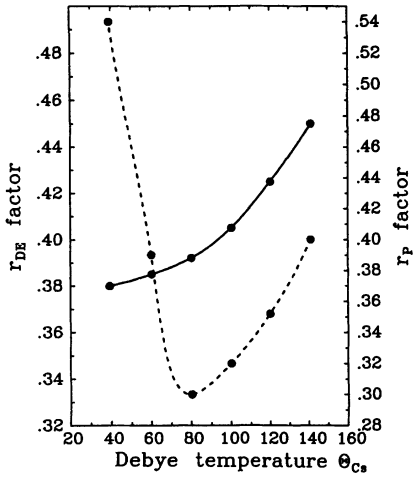

FIG. 5. Sensitivity of r_{DE} (solid line) and r_P factors (dashed line) upon the Debye temperature of cesium.

In the following, $\Theta_D^{Cs} = 80$ K was chosen which value yields minimum values for r_P, while r_{DE} remains essentially unaffected. In order to further confirm the reliability and compatibility of the various r-factor schemes, we performed a crude grid search of the r-factor hypersurface. As Fig. 6 clearly demonstrates, the structural results, connected with the respective minima of r_{DE} and r_P, coincide within the uncertainty of 0.01 Å. According to the curvature of the r-factor plots, an estimation of the "error bars" is accessible and yields ±0.03 Å and ±0.05 Å for the Cs-Ru and the first Ru-Ru layer spacing, respectively.

The final level of agreement between theory and experiment is illustrated in Fig. 7. All major experimental peaks have been reproduced in the calculation. The relative peak intensities of the integer beams are also in good

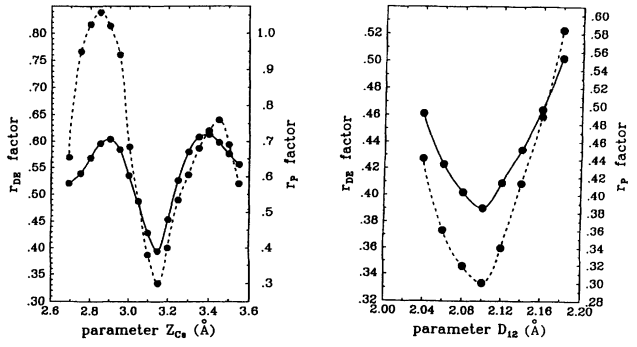

FIG. 6. Dependence of the r factors r_{DE} (solid line) and r_P (dashed line) on the Cs-Ru layer spacing Z_{Cs} and the first Ru interlayer spacing D_{12}.

agreement, while fractional order beams show some deviations, especially for higher electron energies. The associated r factors are $r_P = 0.30$ and $r_{DE} = 0.39$, respectively.

Our results of the LEED analysis are summarized in Fig. 8. In the $(\sqrt{3}\times\sqrt{3})R30°$ phase, Cs occupies the hcp site and can clearly be discriminated from the other high-symmetry adsorption sites. The derived Cs-Ru layer spacing of 3.15 ± 0.03 Å corresponds to a hard-sphere radius of the adsorbed Cs atom of 2.17 ± 0.02 Å, which is equivalent to a Cs-Ru bond length for 3.52 ± 0.02 Å. The Ru-Ru layer spacing equals that value obtained for the clean Ru(0001) surface. Lateral and vertical relaxations of the substrate lead to no further improvement of the structural refinement. Due to the strong dependence of the r_P factor on the Debye temperature of Cs, this quantity can be estimated to a value of 80 ± 10 K. The real part of muffin-tin zero increases from -8 eV for the clean Ru surface to -5 ± 1 eV for the cesiated surface which qualitatively parallels the associated change of the work function.

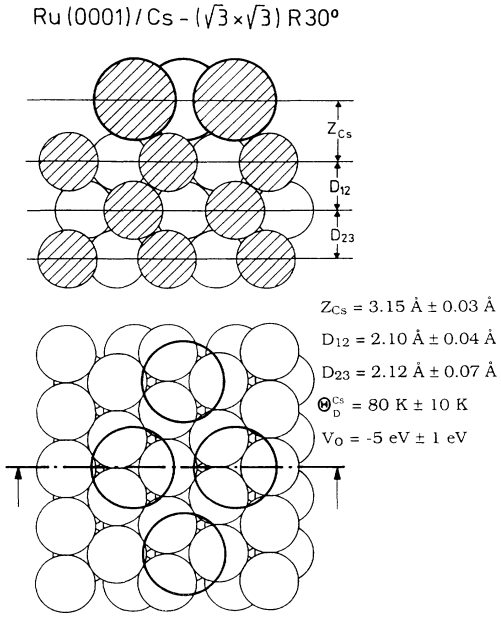

FIG. 8. Structural model of Cs/Ru(0001)-$(\sqrt{3}\times\sqrt{3})R30°$ and the structural parameters for the best-fit arrangement.

C. The (2×2) Cs structure

The Cs (2×2) phase contains again one Cs atom in its overlayer cell. In this LEED structure analysis, five different, highly symmetric adsorption sites were tested: threefold hollow hcp and fcc, on-top, bridge and substitutional site.

The choice of the substitutional adsorption site was prompted by a report favoring this unusual chemisorption geometry in the system Na/Al(111),[43] in which each Na adsorbate kicks out one Al surface atom, creating a six-fold coordinated substitutional site. This geometry is supported by *ab initio* density-functional-theory calculations for several adsorption geometries, showing that the substitutional site has the lowest total energy for the case of Na/Al(111).[43]

The experimental data set contains three integer and five half-order beams in an energy range between 80 and 380 eV. With a step width of 5 eV on the energy scale, a total number of 255 data points was used for comparison with the experiment. To get an overview about distinguished minima in the r-factor hypersurface and suitable starting configurations for an automatic structural refinement, in the first stage of our analysis we performed a coarse-meshed grid search of the parameter space, which was composed of the Cs-Ru and the first Ru-Ru layer spacing; the Debye temperature of Cs was kept fixed at 80 K. The optimum layer spacings and the r factors r_{DE} and r_P for the five competing geometries are listed in Table III. Surprisingly, the on-top adsorption site of cesium reveals a fair preference with respect to the r_P factor. For the threefold hollow sites, the corresponding r factors indicate only a very poor agreement with the experiments. Bridge and substitutional sites belong to the class of indifferent models if judged by their r_P values.

For the five adsorption sites under investigation, we performed an automatic structure refinement whose

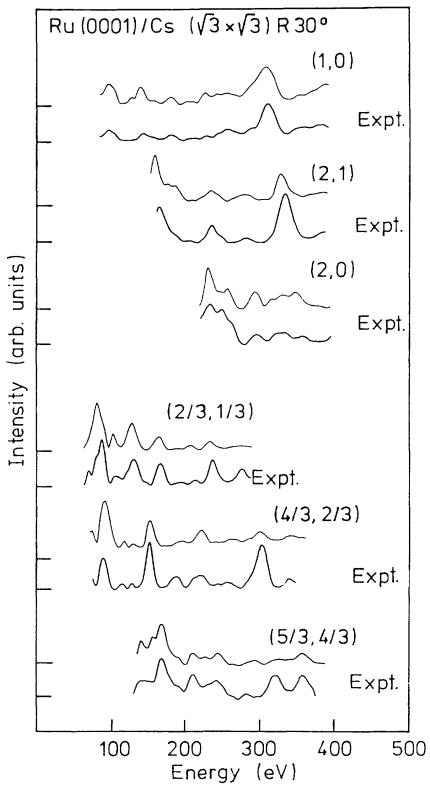

FIG. 7. Comparison of the experimental and calculated best-fit I-E curves for Cs/Ru(0001)-$(\sqrt{3}\times\sqrt{3})R30°$ ($r_P = 0.30$ and $r_{DE} = 0.39$).

TABLE III. r_{DE} factor, r_P (step width 5 eV), and structural parameter for the best-fit arrangement of the respective Cs adsorption sites [(2×2)]. Cs muffin-tin radius of 2.8 Å.

r_{DE}	r_P	Z_{Cs} (Å)	D_{12} (Å)	Adsorption site
0.460	0.700	2.8	2.1	hcp
0.480	0.720	3.3	2.1	hcp
0.520	0.720	3.6	2.1	hcp
0.400	0.513	2.4	2.1	On top
0.440	0.517	2.6	2.1	On top
0.375	0.495	3.2	2.1	On top
0.370	0.504	3.7	2.1	On top
0.361	0.600	2.4	2.1	Bridge site
0.373	0.644	2.9	2.1	Bridge site
0.382	0.672	3.4	2.1	Bridge site
0.413	0.671	3.7	2.1	Bridge site
0.487	0.620	2.4	2.1	fcc
0.496	0.677	3.0	2.1	fcc
0.510	0.712	3.6	2.1	fcc
0.400	0.585	1.9	2.1	Substitutional
0.464	0.707	3.1	2.1	Substitutional

starting configurations are listed in Table III. An additional constraint was that the Cs radius should not become smaller than the ionic radius. Up to eight parameters were simultaneously refined.

Apart from the Ru-Cs and two Ru-Ru interlayer spacings a small buckling of Ru atoms and lateral displacements in the first two layers compatible with the threefold symmetry were considered. The Debye temperature of Cs and the real part of the muffin-tin zero were the nonstructural parameters to be optimized.

Final results were attained after 6–7 iteration cycles, when all parameters attained values within the limits of 0.01 Å, 0.1 eV, and 0.5 K, respectively. A comparison with the exact version showed the same behavior of convergence, however, a reduction in computing time by a factor of 2.9. Common to all adsorption sites, no lateral relaxations of the Ru substrate could be found, and the optimum Debye temperature turned out to be about 30 K. The optimum lattice parameters including the R factor of Pendry r_P and r_{DE} for the respective adsorption geometries are collected in Table IV. These extended calculations show a clear preference for the on-top site. The Ru atoms coordinated with Cs are shifted towards the bulk by 0.10 Å. According to the Ru-Cs layer spacing found for each adsorption geometry, the Ru-Cs bond lengths resulted to be 3.25±0.08 Å (Cs radius =1.90±0.08 Å). Within this uncertainty, the Cs radius is nearly independent of the adsorption site; thus, further discussion about Cs-Ru bonding and Cs radius appears to be decoupled from the question of adsorption site.

Up to now, Cs phase shifts had been used which were calculated with a muffin-tin radius corresponding to the metallic Pauling radius. Our structural results, however, demonstrated a Cs radius reduced by 0.5 and 0.8 Å in the $(\sqrt{3}\times\sqrt{3})R30°$ and (2×2) phase, respectively, which necessitated a recalculation of the phase shifts with a muffin-tin radius of 2.0 Å. Although significant changes were observed in calculated phase shifts, the variation in the corresponding I-E curves was small, leading only to a slight improvement of the r factors r_{DE} and r_P by about 0.05 without any noticeable changes in the structural parameters.

In order to study the dependence of the r factor on the most crucial parameters, we performed a grid search, in which the remaining parameters in each case were kept close to their optimum values. When varying the Debye temperature of Cs, the r factors [Fig. 9(a)] show no pronounced minima but a steep descent for decreasing Θ_D^{Cs} down to 60 K, followed by a nearly flat curve for Debye temperatures below 40 K. The optimum Debye temperature turned out to be 40±10 K. Figure 9(b) illustrates the variation of the r factors with the cesium to ruthenium interlayer spacing. Clearly, both r factors display two distinct minima at 2.70 and 3.15 Å, the deepest minima occurring at 3.15 Å in both cases. We note that adoption of a Ru-Cs layer spacing of 2.70 Å yields an effective cesium radius of 1.35 Å, significantly shorter than the Cs ionic radius, and hence the 2.70 Å value has to be discarded. The optimum outermost ruthenium interlayer spacing [see Fig. 9(c)] was found to be 2.14 Å. Assuming an increase by 0.04 for the r factors to be significant, the resulting parameters are $Z_{Cs}=3.15\pm0.08$ Å and $D_{12}=2.14\pm0.05$ Å. Regarding the magnitude of buckling in the first Ru layer Z_{Ru}, Pendry's r factor [Fig. 9(d)] shows a pronounced minimum at 0.10 Å with an associated uncertainty of ±0.04 Å.

The intensity spectra for the best-fit geometry with an on-top site geometry are displayed in Fig. 10. With exception of the $(\frac{1}{2},0)$ beam, all experimental peaks are well reproduced in the calculations. In order to unravel the poor agreement between theory and experiment for the

TABLE IV. r_{DE} factor, r_P (step width 5 eV), and structural parameter for the best-fit arrangement of the respective Cs sites. Cs phase shifts were calculated for a muffin-tin radius of 2 Å [(2×2)].

r_{DE}	r_P	Z_{Ru} (Å)	Z_{Cs} (Å)	D_{12} (Å)	D_{23} (Å)	Cs radius (Å)	Adsorption site
0.436	0.703	−0.10	2.82	2.08	2.13	1.88	hcp
0.330	**0.390**	**0.10**	**3.15**	**2.14**	**2.13**	**1.90**	**On top**
0.385	0.592	0.01	2.93	2.08	2.16	1.87	Bridge site
0.480	0.662	−0.08	2.95	2.10	2.14	1.96	fcc
0.390	0.570	0.0	1.95	2.06	2.15	1.98	Substitutional

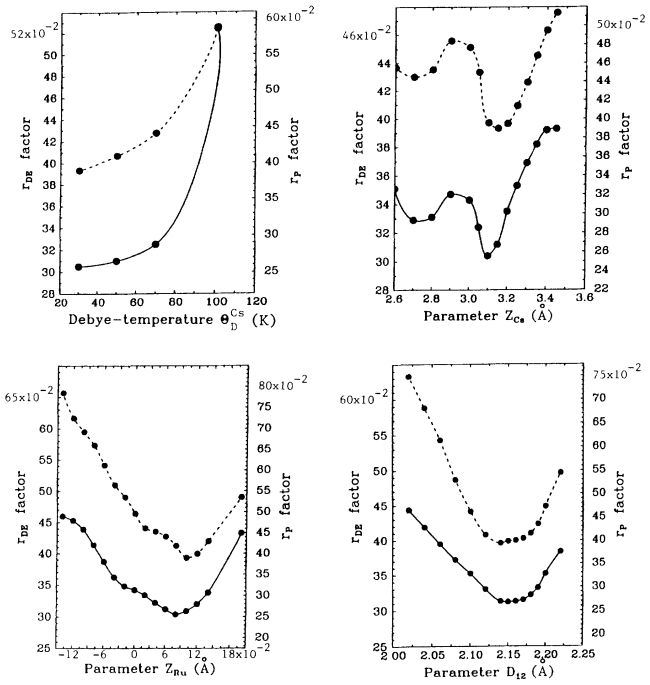

FIG. 9. R-factor behavior (r_{DE}, solid line; r_P, dashed line) as a function of (a) Debye temperature of Cs, (b) Cs-Ru layer spacing Z_{Cs}, (c) magnitude of buckling in the first Ru layer Z_{Ru}, and (d) first Ru interlayer spacing D_{12}.

($\frac{1}{2}$,0) beam, a detailed analysis with the other competing adsorption sites was performed. However, none of these models was able to reproduce satisfactorily the experimental data. For this reason, a further experimental set was measured with particular emphasis put on the ($\frac{1}{2}$,0) beam in order to ascertain that any lack of agreement between theory and experiment was not due to experimental error.

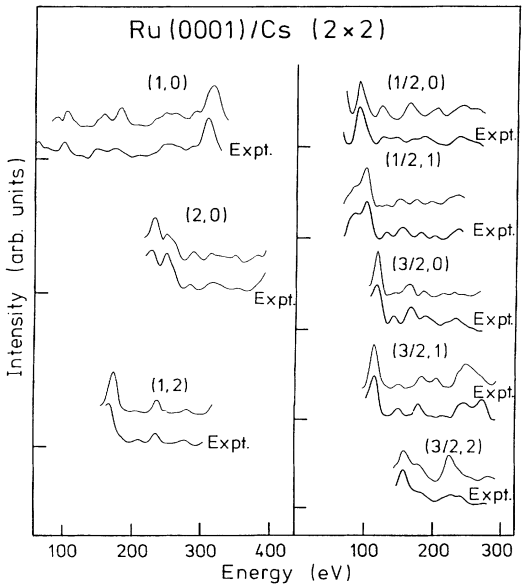

FIG. 10. Comparison of the experimental and calculated best-fit I-E curves for Cs/Ru(0001)-(2×2) (r_P=0.39 and r_{DE}=0.30).

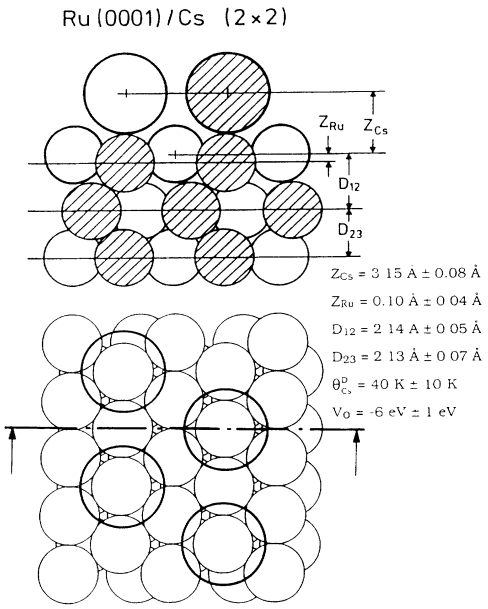

FIG. 11. Structural model of Cs/Ru(0001)-(2×2) and the structural parameters for the best-fit arrangement.

The results of our LEED structure analysis are summarized in Fig. 11. The on-top site of Cs is favored compared to other highly symmetrical adsorption sites. A small shift of 0.10 Å in the Ru atom coordinated with Cs towards the bulk is induced. With the Ru-Cs layer spacing of 3.15±0.08 Å, the Ru-Cs bond length turns out to be 3.25±0.08 Å, which is reduced by 0.27±0.09 Å if compared with the $(\sqrt{3}\times\sqrt{3})R30°$ phase. An optimization of lateral relaxations in the Ru substrate leads to no further improvement of the r factors. The Cs Debye temperature is found to be 40±10 K, which is significantly lower than the corresponding value for the $(\sqrt{3}\times\sqrt{3})R30°$ phase. The real part of the inner potential for the optimum structural model is −6.0±0.5 eV.

VI. DISCUSSION

The nature of the chemisorption bond between alkali-metal atoms and transition-metal surface has been the subject of continuing experimental[4–6,44,45] and theoretical studies.[9,10,46–48] According to Gurney's original picture,[46] the valence s orbital of the alkali-metal atom is broadened and lowered in energy upon interaction with the surface. Consequently, a partial electron transfer to the substrate occurs which effect becomes reduced with increasing coverage due to mutual depolarization of the dipoles formed by the adsorbate complexes, giving rise to the nonlinear variation of the work function with coverage and to a transition of the adsorbed particles from an "ionic" to a more "metallic" state. Although the ongoing discussion on the degree of charge transfer is still controversial and presumably also somewhat semantic in nature, the qualitative concepts are certainly confirmed by the findings for the present system:

Up to Θ=0.15, the work function decreases linearly

with coverage, reflecting a constant dipole moment of about 10 Debye. Then the variation becomes nonlinear and a minimum of $\Delta\phi$ is reached around $\Theta=0.25$ [corresponding to formation of the (2×2) structure], followed by a continuous increase until the value for bulk Cs is reached after completion of the second monolayer. At $\Theta=0.33$ [$\triangleq(\sqrt{3}\times\sqrt{3})R30°$ structure], the dipole moment of the adsorbate complex is smaller than at $\Theta=0.25$ by about 30%. In the present structural analysis, for the (2×2) structure at $\Theta=0.25$, the Ru-Cs bond length was derived to 3.25±0.08 Å. This corresponds to a hard-sphere radius of 1.9 Å for the adparticle, close to its Pauling ionic radius (1.69 Å).[42] For the $(\sqrt{3}\times\sqrt{3})R30°$ structure at $\Theta=0.33$, on the other hand, these values increased to 3.52±0.02 and 2.2 Å, respectively, probably reflecting a more metallic or covalent bonding associated with a smaller dipole moment. These data are in qualitative accordance with the structural parameters for the Cs/Ag(111) system as determined by SEXAFS:[8] Here hard-sphere radii of 1.79 Å at $\Theta=0.15$ and of 2.06 Å at $\Theta=0.3$ were derived. Since it is a general rule that, for ionic bonding, a switching from the coordination number 3 (hcp) to 1 (on-top) results in a decrease in bond length by about 0.3 Å,[49] this straightforward interpretation for the observed change in bond length for the system Cs/Ru(0001) cannot simply be used to quantify the change in ionicity between the two phases. It should be noted, on the other hand, that for the system K/Ni(111), a constant K-Ni layer spacing of 2.7±0.1 Å over the coverage range from $\Theta=0.13$ to 0.28 was reported[50] on the basis of results obtained with the somewhat problematic constant-momentum-transfer averaging (CMTA) LEED technique.[51] It was hence concluded that, with this system, there is no noticeable variation of the nature of the chemisorption bond with coverage. Interestingly, also with the present system the adsorbate-substrate interlayer spacing turns out to be almost the same (taking an uncertainty of 0.05 Å into account) for both ordered phases since these differ in their actual adsorption site geometry. Hence, conclusions based solely on layer spacings may be rather misleading.

The strong decrease of the adsorption energy with coverage as manifested by the large width of the thermal desorption spectra extending over several hundred degrees is unique with alkali-metal overlayers and is generally attributed to the operation of strong dipole-dipole repulsions as a consequence of the large dipole moments. As outlined in the Introduction, dominance of the repulsive interactions between the adsorbates over the corrugation of the substrate potential causes a uniform spreading of the adlayer in a hexagonal geometry which maximizes the A-A distances. In the absence of long-range order at low coverages, diffraction rings were frequently observed in the LEED pattern whose radii expand continuously with increasing coverage.[52] The occurrence of the same phenomenon with the present system for $\Theta\leq0.17$ indicates indeed that the corrugation of the substrate potential is fairly weak, otherwise lattice-gas structures with unit cells larger than (2×2) would be expected for lower coverages as reported in other cases.[19] This means, on the other hand, that the differences in the A-S potential in different adsorption sites are relatively small, so that an inherently less favorable site might nevertheless be occupied due to overcompensation by the gain in interaction energy. This conclusion is further supported by the observation of structures with rotated unit cells, reflecting even occupation of out-of-registry adsorption sites, in the transition region between the (2×2) and $(\sqrt{3}\times\sqrt{3})R30°$ phases.

For alkali-metal atoms (like for other atomic adsorbates) generally a preference of sites with the highest possible coordination is found.[53] For the present system this would be the hcp threefold hollow site which is indeed also derived for the $(\sqrt{3}\times\sqrt{3})R30°$ phase. However, for the (2×2) phases formed by Cs/Cu(111) (Ref. 54) and K/Ni(111) (Ref. 55) occupation of on-top sites was derived as for the (2×2) structure of the present system. [On-top site adsorption was also found for Xe/Pt(111),[56] but in this case the nature of the adsorption bond is *certainly* different from that for alkali-metal chemisorption.] The Cs/Ru(0001) system investigated here exhibits, however, a peculiar behavior in so far as *different* sites are occupied in the (2×2) and $(\sqrt{3}\times\sqrt{3})R30°$ structures. Both phases are commensurate with the substrate lattice and would permit identical adsorption site geometries without affecting the unit cell symmetry, i.e., the mutual configurations of the adparticles. Although their interactions are dominated by dipole-dipole repulsions, we have hence to conclude that these are not solely dependent on the adatom-adatom separation r, but also on the adsorption site geometry, and hence the S-A and A-A potentials are no longer separable.

For this phenomenon the following qualitative explanation is offered: The interaction energy between two dipoles μ *at a metal surface* is proportional to $(\mu^2/r^3)\exp(-r/l_s)$, where l_s is the effective Thomas-Fermi charge screening length as "seen" by the dipoles. l_s, and hence also the dipole-dipole repulsion, decreases with the effective conduction electron densities between the two dipoles.[57,4] A similar effect is seen in the calculations of the electrostatic potential caused by adsorbates on jellium surfaces.[58] Inspection of Fig. 11 shows that, in the (2×2) phase, better screening between the dipoles can be achieved if neighboring alkali-metal adatoms have a substrate atom directly between them as can be realized with occupation of on-top sites, but not with hollow sites. The fact that these substrate atoms between the adatoms are raised by 0.12 Å in the K/Ni(111) system[55] and by 0.10 Å in the Cs/Ru(0001) system (this work) leading to an enhancement of their screening ability, is consistent with this model. As can be seen from Fig. 8, with the $(\sqrt{3}\times\sqrt{3})R30°$ phase, occupation of on-top sites would no longer improve the screening, and instead now the hollow sites are preferred.

With the $c(2\times2)$ phases formed for alkalis on fcc(100) surfaces, generally the hollow sites are occupied.[4] Again, in these structures a substrate atom is located between neighboring adparticles, which, according to our model, helps to screen adatom-adatom repulsions. An interesting case is offered by the $c(4\times2)$ phase formed with Cs/Rh(100) where again hollow sites are occupied,[52(c)] although Cs-Cs nearest-neighbor repulsions would be more

effectively screened for on-top sites within our model. However, in that structure one finds that the Cs-Cs next-nearest-neighbor distance is only slightly longer than the Cs-Cs nearest-neighbor distance, but there are twice as many of the former (next-nearest-neighbor) interactions occurring in the adlayer. These are more effectively screened for the choice of hollow sites over on-top sites, since *two* substrate atoms sit almost directly between two such next-nearest-neighbor hollow sites, whereas the space between two such on-top sites is somewhat more open (i.e., less effectively screened). As a consequence, the difference in repulsive interactions between on-top and hollow site occupation might become minimal, and the *a priori* preference for the hollow sites may win out here.

In general, the actual adsorption site occupied in adsorption systems of the type under discussion will be the result of a sensitive balance between corrugation of the substrate potential, magnitude of the dipole moment, interatomic spacing, and electrostatic screening, and therefore no general rules can be formulated *a priori.*

ACKNOWLEDGMENTS

The authors gratefully acknowledge fruitful discussions with R. Diehl, J. Neugebauer, and M. Scheffler as well as technical assistance by E. Piltz. C.T.C. acknowledges partial support for this work by the U.S. National Science Foundation.

*Permanent address: Deutsches Patentamt, München, FRG.

[1]See, e.g., J. M. Mac Laren, J. B. Pendry, P. J. Rous, D. K. Saldin, G. A. Somorjai, M. A. Van Hove, and D. D. Vvedensky, *Surface Crystallographic Information Service* (Reidel, Dordrecht, 1987).

[2]B. N. J. Persson, M. Tüshaus, and A. M. Bradshaw, J. Chem. Phys. **92**, 5034 (1990).

[3]M. Tüshaus, W. Berndt, H. Conrad, A. M. Bradshaw, and B. Persson, Appl. Phys. A **51**, 91 (1990).

[4]C. T. Campbell, Annu. Rev. Phys. Chem. **41**, 775 (1990).

[5]E. Bauer, in *The Chemical Physics of Solid Surfaces and Heterogeneous Catalysis,* edited by D. A. King and D. P. Woodrüff (Elsevier, Amsterdam, 1984), Vol. 3, Part B, p. 1.

[6]*Physics and Chemistry of Alkali Metal Adsorption,* edited by H. P. Bonzel, A. M. Bradshaw, and G. Ertl, Materials Science Monographs (Elsevier, Amsterdam, 1989), Vol. 57.

[7]I. Langmuir and K. H. Kingdon, Phys. Rev. **21**, 380 (1923).

[8]G. M. Lamble, R. S. Brooks, D. A. King, and D. Norman, Phys. Rev. Lett. **61**, 1112 (1988).

[9](a) H. Ishida, Phys. Rev. B **38**, 8006 (1988); (b) **39**, 5492 (1989); (c) **40**, 1341 (1989).

[10]M. Scheffler, Ch. Droste, A. Fleszar, F. Máca, G. Wachutka, and G. Barzel, Physica B **172**, 143 (1991).

[11]K. Wandelt, H. Hulse, and J. Küppers, Surf. Sci. **104**, 212 (1981).

[12]K. Heinz, Prog. Surf. Sci. **27**, 239 (1988).

[13]H. Bludau, H. Over, M. Skottke-Klein, and G. Ertl (unpublished).

[14]S. Chandavarkar and R. D. Diehl, Phys. Rev. B **38**, 12 112 (1988).

[15]J. Hrbek, Surf. Sci. **164**, 139 (1985).

[16]A. Simon, W. Brämer, B. Hillenköotter, and H. J. Kullmann, Z. Anorg. Allg. Chem. **419**, 253 (1976).

[17]F. D. Rassini *et al., Selected Values of Chemical Thermodynamic Properties,* Natl. Bur. Stand. Circ. No. 500 (U.S. GPO, Washington, D.C., 1952).

[18]D. L. Doering and S. Semancik, Surf. Sci. **129**, 177 (1983).

[19]G. Pirug and H. P. Bonzel, Surf. Sci. **194**, 159 (1988).

[20]C. G. Shaw, S. C. Fain, Jr., and M. D. Chinn, Phys. Rev. Lett. **41**, 955 (1979).

[21]S. Calisti, J. Suzanne, and J. A. Venables, Surf. Sci. **115**, 455 (1982).

[22]S. C. Fain, Jr., M. D. Chinn, and R. D. Diehl, Phys. Rev. B **21**, 4170 (1980).

[23]T. Aruga, H. Tochihara, and Y. Murata, Phys. Rev. Lett. **52**, 1794 (1984).

[24]D. L. Doering and S. Semancik, Phys. Rev. Lett. **53**, 66 (1984).

[25]A. D. Novaco and J. P. McTague, Phys. Rev. Lett. **38**, 1286 (1977).

[26]J. P. McTague and A. D. Novaco, Phys. Rev. B **19**, 5299 (1979).

[27]R. Duszak and R. H. Prince, Surf. Sci. **226**, 33 (1990).

[28]S. Y. Tong and M. A. Van Hove, Phys. Rev. B **16**, 1459 (1977).

[29](a) J. Rundgren und A. Salwen, J. Phys. C **7**, 4247 (1974); (b) **9**, 3701 (1976).

[30]W. Moritz, J. Phys. C **17**, 353 (1983).

[31]K. Schwarz, Theor. Chim. Acta (Berlin) **34**, 225 (1975).

[32](a) R. Feder and W. Moritz, Surf. Sci. **77**, 505 (1978); (b) D. A. Liberman, Phys. Rev. **171**, 1 (1968); (c) D. A. Liberman, D. T. Cromer, and J. T. Waber, Comput. Phys. Commun. **2**, 107 (1971).

[33]*International Tables for X-Ray Crystallography,* edited by C. H. MacGillavry and G. D. Rieck (Kynoch, Birmingham, 1962), Vol. III.

[34]G. Kleinle, W. Moritz, D. L. Adams, and G. Ertl, Surf. Sci. **219**, L637 (1989).

[35]G. Kleinle, W. Moritz, and G. Ertl, Surf. Sci. **238**, 119 (1990).

[36]G. Kleinle, Ph.D. thesis, Freie Universität, Berlin, 1989.

[37](a) W. Moritz, H. Over, G. Kleinle, and G. Ertl, in *The Structure of Surfaces III,* edited by M. A. Van Hove, S. Y. Tong, and Xie Xide (Springer, Berlin, 1991), p. 128; (b) H. Over, H. Bludau, U. Ketterl, M. Skottke-Klein, W. Moritz, and G. Ertl (unpublished).

[38]H. Over, U. Ketterl, G. Kleinle, W. Moritz, and G. Ertl (unpublished).

[39]G. Michalk, W. Moritz, H. Pfnür, and D. Menzel, Surf. Sci. **129**, 92 (1983).

[40]E. Zanazzi and F. Jona, Surf. Sci. **62**, 61 (1977).

[41]J. B. Pendry, J. Phys. C **13**, 937 (1980).

[42]L. Pauling, *The Nature of the Chemical Bond,* 3rd ed. (Cornell University Press, Ithaca, 1960).

[43]A. Schmalz, S. Aminpirooz, L. Becker, J. Haase, J. Neugebauer, M. Scheffler, D. R. Batchelor, D. L. Adams, and E. Bøgh, Phys. Rev. Lett. **67**, 2163 (1991).

[44]M. L. Shek, J. Hrbek, T. K. Sham, and G. Q. Xu, Phys. Rev. B **41**, 3447 (1990).

[45]D. M. Riffe, G. K. Wertheim, and P. H. Citrin, Phys. Rev. Lett. **64**, 571 (1990).

[46]R. W. Gurney, Phys. Rev. **47**, 2798 (1935).
[47]E. Wimmer, A. J. Freeman, M. Weinert, H. Krakauer, J. R. Hiskes, and A. M. Karo, Phys. Rev. Lett. **48**, 1128 (1982).
[48]H. Ishida, Surf. Sci. **242**, 341 (1991).
[49]C. Kittel, *Introduction to Solid State Physics,* 5th ed. (Wiley, New York, 1976), p. 101.
[50]D. Fisher, Zi-You Li, and R. D. Diehl, Surf. Sci. **259**, 85 (1991).
[51]M. G. Lagally, T. C. Ngoc, and M. B. Webb, Phys. Rev. Lett. **26**, 1557 (1971).
[52](a) W. C. Fan and A. Ignatiev, Phys. Rev. B **37**, 5274 (1988); **39**, 6816 (1990); (b) C. T. Campbell, J. Phys. Chem. **89**, 5789 (1985); (c) S. Andersson and B. Kasemo, Surf. Sci. **32**, 78 (1972); (d) R. L. Gerlach and T. N. Rhodin, *ibid.* **17**, 32 (1969); (e) J. Cousty, R. Riwan, and P. Soukiassian, *ibid.* **152/153**, 297 (1985).
[53](a) J. E. Demuth, D. W. Jepsen, and P. M. Marcus, J. Phys. C **8**, L25 (1975); (b) S. Andersson and J. B. Pendry, Solid State Commun. **16**, 563 (1975); (c) B. A. Hutchins, T. N. Rhodin, and J. E. Demuth, Surf. Sci. **54**, 419 (1976); (d) M. A. Van Hove, S. Y. Tong, and N. Stoner, *ibid.* **54**, 259 (1976); (e) N. V. Smith, H. H. Farrell, M. M. Traum, D. P. Woodruff, D. Norman, M. S. Woolfson, and B. W. Holland, Phys. Rev. B **21**, 3119 (1980); (f) C. V. Eggeling, G. Schmidt, G. Besold, L. Hammer, K. Heinz, and K. Müller, Surf. Sci. **221**, 11 (1989); (g) C. J. Barnes, P. Hu, M. Lindroos, and D. A. King, *ibid.* **251/252**, 561 (1991).
[54]S. A. Lindgren, L. Walldén, J. Rundgren, P. Westrin, and J. Neve, Phys. Rev. B **28**, 6707 (1983).
[55]D. Fisher, S. Chandavarkar, I. R. Collins, R. D. Diehl, P. Kaukasoina, and M. Lindroos (unpublished).
[56](a) K. Kern, R. David, R. L. Palmer, and G. Comsa, Phys. Rev. Lett. **56**, 620 (1986); (b) J. M. Gottlieb, Phys. Rev. B **42**, 5377 (1990).
[57]N. W. Ashcroft and N. D. Mermin, *Solid State Physics* (Holt, Rinehart & Wilson, New York, 1976), p. 342.
[58]N. D. Lang, S. Holloway, and J. K. Nørskov, Surf. Sci. **150**, 24 (1985).

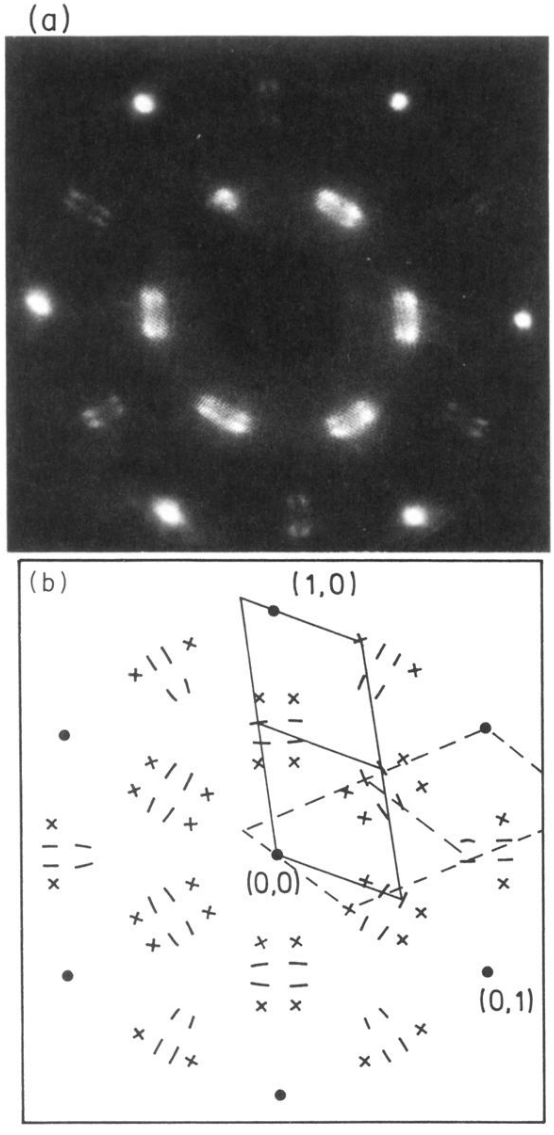

FIG. 3. Photograph of the LEED pattern for $\Theta_{Cs}=0.27$ ($E=55$ eV) together with a schematical picture. For clarity, only one of the possible unit cells (solid lines) and corresponding unit cells due to double scattering (dashed lines) is inscribed. Weak spots are marked by crosses.